Sensors and Materials, Vol. 35, No. 10 (2023) 4571–4584
MYU Tokyo

S & M 3415

State Synchronous Control for Nerve-cell Systems via Adaptive Faster Finite-time-stabilized Sliding Mode Method

Ruizhao Yang,[1,2] Chi-Hsin Yang,[1*] Chuanjian Liang,[1]
Kun-Chieh Wang,[1] and Hong-Yi Chen[1]

[1]School of Physics and Telecommunication Engineering, Yulin Normal University,
Yulin City, Guang Xi, 53700, China
[2]School of Physical Science and Technology, Guangxi Normal University,
Guilin City, Guang Xi, 541004, China

(Received April 7, 2023; accepted September 22, 2023)

Keywords: adaptive control, state synchronous control, finite-time stabilization, FitzHugh–Nagumo nerve-cell model, neuronal circuit, sliding mode.

Using a novel integral-type faster finite-time-stabilized sliding mode (IFFSSM), we developed an adaptive control scheme for solving the state synchronous control problem for two space-clamped FitzHugh–Nagumo (SFHN) nerve-cell systems under the influence of disturbances. Because of the characteristics of the SFHN nerve-cell model under the principle of electrochemistry, the special stability property of IFFSSM is that two state variables of the system are stabilized in sequence on the sliding surface. Two theorems of the stability were also provided and proven. Numerical experiments were performed. The performance of the proposed control method was validated for the future practical application to neuronal circuits.

1. Introduction

Since the chaotic state synchronous control problem was introduced, it has attracted much attention owing to the broad range of applications in many research fields such as secure communication,(1) encryption,(2) circuits,(3) biomedical systems,(4) micro-electro-mechanical systems,(5,6) nervous systems,(7,8) and signal encoding and transmission.(9–11) Chaotic state synchronization is the matching of the states between two chaotic systems that start from different initial conditions. In recent years, state synchronization of the nerve-cell system, which is conducive to gaining a good comprehension of the behaviors of nerve cells, has been widely investigated.(7,8,12–22)

In the past, chaotic behaviors were studied using various nerve models such as the Hodglein–Huxley (HH) model,(23) the Hindmarsh–Rose model,(24) and the FitzHugh–Nagumo (FHN) models.(25–27) The HH nerve-cell model(23) is a more complete differential equation model for describing the dynamics of a nerve-cell's membrane voltage. For practical application, the space-clamped FHN (SFHN) nerve cell(27) is more convenient for investigating the dynamics of a

*Corresponding author: e-mail: yang2020@ylu.edu.cn
https://doi.org/10.18494/SAM4451

ISSN 0914-4935

nerve cell. The typical work of studying chaos and bifurcation of the SFHN nerve-cell model was addressed in Refs. 12 and 28.

The architecture of circuit-implemented neuron systems was described in Ref. 29. The frontier viewpoint is that the establishment of neuronal circuits, based on the behavior of the nerve cell system, can give rise to new application themes in artificial intelligence. It highlights the importance of developing neuronal circuit systems. Moreover, quick adaptability is demanded of artificial nerve-cell network systems to accommodate unpredictable environments. Machine learning technologies are applied to overcome the difficult and complex issues of such systems.[30] FHN neuronal circuits have been constructed of, for example, simple circuits,[31] feedback circuits consisting of operational amplifiers and resistors,[32] field programmable gate arrays,[33] and field-effect transistors (FET).[34] Furthermore, on the framework of the traditional FHN nerve-cell system, many new types of FHN neuronal circuit system have been proposed, such as the photosensitive neuron,[22,35] the thermosensitive neuron,[36] the piezoelectric neuron,[37] and the neuronal circuit systems with electromagnetic induction.[38–40] Such new types of neuronal circuit contribute to the development of multidiscipline applications in science and technology. The implementation of neuronal circuits in the development of a novel control system design for nerve cells makes engineering sense. It will be effective in the operation of novel and more practical FHN neuronal circuit control systems with voltage-sensing equipment.

A single SFHN nerve-cell model subject to an external electric stimulation (EES), as applied in the firing of a nerve cell, is defined by the differential equations vs the nondimensional time τ,[12]

$$\begin{cases} \dot{u}_1 = -u_1^3 + (a+1)u_1^2 - au_1 - v_1 + I_0 + I_m \cos(\omega_m \tau), \\ \dot{v}_1 = -b(v_1 - cu_1), \end{cases} \tag{1}$$

where the state variable u_1 is the rescaled activation potential and v_1 denotes the rescaled recovery voltage.[27] The positive constants *a, b, c* dominate the behavior of Eq. (1) where $I_m\cos(\omega_m\tau)$ is an EES with amplitude I_m and frequency $f = \omega_m/2\pi$, and I_0 is an ionic current in the nerve cell. An individual SFHN nerve-cell model with an EES is expected to exhibit a variety of behaviors. It is reported that the nerve-cell model displays complicated chaotic firing for certain values of I_m.[12,28] Otherwise, the dynamics of the SFHN nerve-cell model are susceptible to the variation of the ionic current and the EES signal frequency. With the typical system parameters of $a = 0.25$, $b = 0.02$, $c = 0.25$, $I_m = 0.055$, $I_0 = 0.082$, and $\omega_m = 0.1$, the SFHN nerve-cell model shows chaotic dynamics.[12]

In previous studies, the problem of chaotic control in a SFHN nerve-cell model has been addressed using an adaptive passive control method.[12] A variety of schemes such as adaptive control, back-stepping control, and LMI-based adaptive control technologies have been introduced for state synchronizations between two SFHN nerve cells under EES.[13–15] By considering different EESs and ionic currents between two individual SFHN nerve cells, state synchronization was achieved,[7] and the adaptive sliding mode control (SMC) with robustness was proposed. Lu and Chen[8] developed SMC with an input–output linearized approach. For

coupled FHN nerve-cell networks, synchronization was achieved by Zhang[17] using a typical robust SMC scheme with adaptive time-delay feedback control, and Ibrahim *et al.*[20] achieved lag synchronization using a feedback control scheme. For the new types of FHN nerve-cell systems, finite-time synchronization of two dual-memristor-based networks was introduced.[21] State coupling synchronization was developed by Zhang *et al.*[18] and phase synchronization was developed by Zhang *et al.*[19] and Hussain *et al.*[22] for photosensitive FHN neurons.

This study is motivated by the following observations. In state synchronization between two SFHN nerve cells, the main idea of SMC reported in past studies is to force the error state trajectory to arrive at and stay on the sliding surface, which, in Ref. 7, was a line with a negative slope, and in Ref. 5, a bending curve, in the phase plane. Then, the error states simultaneously converge to the origin along the defined sliding surface. Finally, a satisfactory performance of control was obtained by applying the proposed control scheme. In the mathematical model of the SFHN nerve cell system shown in Eq. (1), it describes that recovery voltage v_1 is induced by the activation potential u_1 under the principles of electrochemistry. That is, $\dot{v}_1 + bv_1 = bcu_1$. Motivated by this, we define a novel sliding mode (SM) to develop an adaptive SMC scheme to achieve state synchronization between two SFHN nerve cells in this study. The novel SM is defined as having stability such that, on the sliding surface, the error of the activation potential first converges to and remains at zero in a finite time. Then, according to the second equation of Eq. (1), the error of the recovery voltage is also exponentially stable.

The novelty and contributions of this study are as follows.

(1) Unlike the past works on the SMC scheme,[5,7] the novel integral-type faster finite-time-stabilized SM (IFFSSM), which is defined by the proportional, fractional powered, and integral terms of two state variables, has the property that two state variables are stabilized in sequence. That is, a state variable is finite-time stabilized in advance and the other state variable is subsequently exponentially stabilized on the sliding surface. This leads to a special shape of the sliding surface defined by the IFFSSM that promotes stability. The details of the stability are proven by the provided Theorem 1 in Sect. 3.
(2) To control the state synchronization between two SFHN nerve cells, the robust novel adaptive SMC scheme based on the IFFSSM is performed in accordance with Theorem 2 in Sect. 3. The main idea of the developed control scheme is divided in two parts. First, the error state trajectory is controlled to arrive at and remain on the sliding surface defined by the IFFSSM. Second, on the basis of the stable property of the IFFSSM, the error of the activation potential tends to and remains at zero at a finite time in advance. Then, the error of the recovery voltage is exponentially stabilized in sequence.
(3) Three state-feedback gains are included in the proposed adaptive IFFSSM control scheme to cope with nonlinear dynamics without eliminating any nonlinear terms. Meanwhile, the three gains are updated online adaptively using an established algorithm. The stable state synchronization is presented on the basis of the Lyapunov stability theory.
(4) The validation and feasibility of the developed control scheme are verified by numerical simulations. They can mainly support the future implementation of neuronal circuits. In Sect. 4, the numerical experiments we performed are described. The performance of the proposed scheme is further checked. Although, in accordance with the stable properties of

the IFFSSM, the error states are stabilized in sequence in the simulation results, by tuning the parameter involved in the proposed control scheme, the two error states are almost simultaneously converged to the origin in the phase plane. However, the almost simultaneous convergence leads to a good control performance of state synchronization. The details are given in Sect. 4.

The content of the study is summarized. In Sect. 2, the state synchronous control problem for two SFHN nerve cells is formulated. In Sect. 3, the definition of the novel IFFSSM and its stable property are provided. In addition, the concept of the design and the proof of stability of the adaptive IFFSSM control scheme are described. In Sect. 4, the numerical experiments are discussed, and the conclusions are presented.

2. Definition of State Synchronous Control Problem

The state synchronous control problem between two SFHN nerve cells is formulated by regarding the different EESs and I_0. The master SFHN nerve cell is defined by Eq. (1) by adding an external disturbance, $d(\tau)$, and a system uncertainty, $\Delta(u_1, v_1)$. The slave SFHN nerve cell is also formulated as Eq. (1) with the addition of the input $\phi(\tau)$, and is modeled as

$$\begin{cases} \dot{u}_2 = -u_2^3 + (a+1)u_2^2 - au_2 - v_2 + I_{0\_s} + I_s \cos(\omega_s \tau) + \phi(\tau), \\ \dot{v}_2 = -b(v_2 - cu_2), \end{cases} \tag{2}$$

where u_2, v_2 are the state variables. $I_s\cos(\omega_s\tau)$ is the EES with amplitude I_s and frequency $f_s = \omega_s/2\pi$, and I_{0_s} is the ionic current. In the control problem of this study, the two EESs and two different I_0 in Eqs. (1) and (2) are considered. We set $I_{0\_s} \neq I_0$, $I_s \neq I_m$, $\omega_s \neq \omega_m$. Furthermore, we assume that the master and slave nerve cells of Eqs. (1) and (2), respectively, have unique solutions in the time interval $\tau \in [0, \infty)$ for any given initial condition. Both SFHN nerve cells still show the behavior of bounded state trajectories under the influences of external disturbance $d(\tau)$, system uncertainty $\Delta(u_1, v_1)$, and designed control $\phi(\tau)$.

The synchronous error states are defined as

$$\theta_u(t) = u_2(t) - u_1(t), \theta_v(t) = v_2(t) - v_1(t). \tag{3}$$

The control scheme $\phi(t)$ in Eq. (2) is proposed for the state synchronous control problem so that for given different initial conditions of nerve cells of Eqs. (1) and (2), the responses of the slave nerve cell approach those of the master nerve cell.

By taking the time derivative of Eq. (3), the dynamical system of the synchronous error states is obtained as

$$\begin{cases} \dot{\theta}_u = [-F_1(u_1,u_2) + F_2(u_1,u_2)]\theta_u - a\theta_u - \theta_v + (I_{0\_s} - I_0) \\ \qquad + I_s \cos(\omega_s \tau) - I_m \cos(\omega_m \tau) - \Delta(u_1, v_1) - d(\tau) + \phi(\tau), \\ \dot{\theta}_v = -b(\theta_v - c\theta_u), \end{cases} \tag{4}$$

where $F_1(u_1, u_2) = u_1^2 + u_1u_2 + u_2^2$ and $F_2(u_1, u_2) = (a + 1)(u_1 + u_2)$ are bounded nonlinear functions owing to both the master and slave nerve cells being chaotic with bounded phase trajectories of state variables. In the design of the control scheme, $F_1(u_1, u_2)$ and $F_2(u_1, u_2)$ are treated as variable gains of $\theta_u(\tau)$ and are assumed to have upper bounds and to satisfy

$$0 < \left|F_1(u_1,u_2)\right| \le M_1, 0 < \left|F_2(u_1,u_2)\right| \le M_2. \tag{5}$$

Definition 1:

The accomplishment of state synchronization between the two SFHN nerve cells of Eqs. (1) and (2) is equivalent to the synchronous error states in Eq. (4) approaching zero. This means that $\lim_{\tau\to\infty} \left|\theta_u(\tau)\right| \to 0$ and $\lim_{\tau\to\infty} \left|\theta_v(\tau)\right| \to 0$.

3. Design of Adaptive Integral-type Sliding Mode Control

It has been shown that the state synchronous control problem is altered to stabilize the dynamical system by Eq. (4) by applying the appropriate control scheme $\phi(\tau)$. On the basis of the definition of IFFSSM, an adaptive control scheme for solving the state synchronous control problem between two SFHN nerve cells is developed in this section. To develop the main theorem, the lemma of finite-time stability is provided in advance.

Lemma:[41]

For the nonlinear differential equation

$$s(\tau) = \dot{x}(\tau) + \rho x(\tau) + \lambda \left[x(\tau)\right]^{n/m} = 0, \tag{6}$$

where $\lambda > 0$, $\rho > 0$, the positive n, m are odd integers that satisfy $0 < n/m < 1$. If $\forall x(\tau = 0) = x_0 \neq 0$, $x(\tau)$ can reach the origin $x = 0$ at the fixed time of

$$T_s = \frac{m}{\rho(m-n)} \ln\left[\frac{\rho\left(x_0\right)^{(m-n)/m}}{\lambda} + 1\right] > 0\,, \tag{7}$$

and remain there for $\forall \tau \ge T_s > 0$. Then, this state $x(\tau)$ is globally finite-time stable.

Equation (6) is the definition of the faster terminal sliding surface in Ref. 41. The origin $x = 0$ is a terminal attractor. The proof of the lemma is omitted here but can be found in Ref. 41.

The concept for developing the adaptive IFFSSM control scheme is described in sequence. Firstly, an IFFSSM $\sigma(\tau)$ is introduced and the finite-time stability of $\sigma(\tau) = 0$ is proven. Secondly, on the basis of the IFFSSM, the adaptive control scheme is developed such that, in the phase plane, the synchronous error states $\theta_u(t)$ and $\theta_v(t)$ are forced to maintain $\sigma(\tau) = 0$ and $\dot{\sigma}(\tau) = 0$ under the influence of internal and external disturbances.

Definition 2:

The definition of the novel IFFSSM $\sigma(\tau)$ is given by

$$\sigma(\tau) = [\theta_u(\tau)]^{p/q} + \alpha \int_{t=0}^{\tau} [\theta_u(t)]^{p/q} dt + \frac{\beta}{c}\left[\frac{1}{b}\theta_v(\tau) + \int_{t=0}^{\tau} \theta_v(t) dt\right], \tag{8}$$

where $\alpha, \beta > 0$ and positive p and q are odd integers with $1 < p/q < 2$.

The introduced SM is defined by the proportional, fractional powered, and integral terms of $\theta_u(t)$ or $\theta_v(t)$, and the finite-time stability of the IFFSSM on the sliding surface $\sigma(\tau) = 0$ is obtained in accordance with the following Theorem 1.

Theorem 1.

For the second equation of Eq. (4) with the IFFSSM $\sigma(\tau)$ in Eq. (8), the synchronous error state $\theta_u(\tau)$ is globally finite-time stable with $\sigma(\tau) = 0$ and $\dot{\sigma}(\tau) = 0$. The finite time τ_s taken for $\theta_u(\tau)$ to approach the origin $\theta_u = 0$ and remain there, $\forall \tau \geq \tau_s > 0$, is given by

$$\tau_s = \frac{p}{\alpha(p-q)} \ln\left(\frac{\alpha}{\beta}\left[\theta_u(\tau_0)\right]^{(p-q)/q} + 1\right) + \tau_0, \tag{9}$$

where $\tau = \tau_0 > 0$ is the time at which the synchronous error states $\theta_u(t)$, $\theta_v(t)$ arrive at the sliding surface $\sigma(\tau) = 0$. Then, the synchronous error state $\theta_v(\tau)$ is exponentially stabilized.

Proof.

For the given $\theta_u(0)$, $\theta_v(0)$, when the synchronous error states $\theta_u(t)$ and $\theta_v(t)$ reach the sliding surface $\sigma(\tau) = 0$ with $\dot{\sigma}(\tau) = 0$, the dynamical system in Eq. (8) with the second equation in Eq. (4) is equivalently altered as

$$\begin{aligned} &\dot{\sigma}(\tau) = \frac{p}{q}\left[\theta_u(\tau)\right]^{(p/q)-1} \dot{\theta}_u(\tau) + \alpha\left[\theta_u(\tau)\right]^{(p/q)-1} + \frac{\beta}{c}\left[\frac{1}{b}\dot{\theta}_v(\tau) + \theta_v(\tau)\right] = 0 \\ &\Rightarrow \frac{d\theta_u(\tau)}{d\tau} + \frac{\alpha q}{p}\theta_u(\tau) + \frac{\beta q}{p}\left[\theta_u(\tau)\right]^{2-(p/q)} = 0, \end{aligned} \tag{10}$$

where $1 < p/q < 2$ and $0 < 2 - (p/q) < 1$. The corresponding initial condition is $\theta_u(\tau_0) \neq 0$, where $\tau_0 > 0$ is the time of $\theta_u(t)$ and $\theta_v(t)$ in Eq. (4) to reach $\sigma(\tau) = 0$ from the given $\theta_u(0)$, $\theta_v(0)$.

In accordance with the aforementioned lemma, by replacing the corresponding parameters with $\lambda = \beta q/p$, $\rho = \alpha q/p$, $n/m = 2 - (p/q)$, we obtain the finite-time stability of $\theta_u(\tau)$. The finite time τ_s for approaching the origin $\theta_u = 0$ and holding constant $\forall \tau \geq \tau_s > 0$ is calculated using Eq. (9). Then, it is quite clear that $\theta_v(\tau)$ is exponentially stabilized for $\theta_v(\tau_s) \neq 0$ under $\theta_u = 0$, $\forall \tau \geq \tau_s > 0$. That is,

$$\frac{1}{b}\dot{\theta}_v(\tau) + \theta_v(\tau) = 0 \Rightarrow \theta_v(\tau) = \theta_v(\tau_s)\exp(-b\tau), \forall \tau \geq \tau_s > 0, b > 0. \tag{11}$$

This proves Theorem 1.

Remark 1.

From Theorem 1, the sliding surface $\sigma(\tau) = 0$ defined by the IFFSSM has a special shape. For various sets of α, β, the shapes of sliding surfaces are shown in Fig. 1.

Remark 2.

The value of the finite time τ_s in Eq. (9) is mainly caused by tuning the parameter $\alpha > 0$. In addition, the performance of the controlled system depends on the chosen value of $\alpha > 0$, as discussed in Sect. 4.

On the basis of the IFFSSM in Eq. (8), the adaptive control with the corresponding adaption algorithms is designed in Theorem 2 by taking into account the existence of system uncertainty and external disturbance.

Theorem 2.

On the basis of the defined IFFSSM $\sigma(\tau)$ in Eq. (8), the control input in Eq. (4) is designed in the form of $\phi(\tau) = \phi_{eq}(\tau) + \phi_{sw}(\tau)$, where

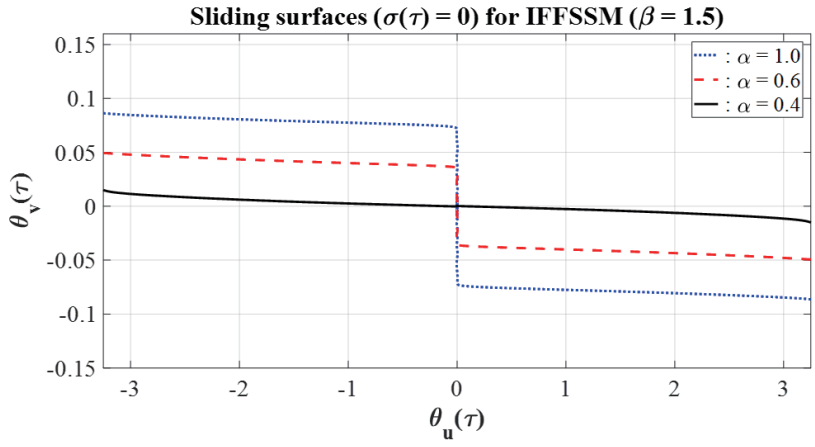

Fig. 1. (Color online) Shapes of sliding surfaces $\sigma(\tau)$ for various sets of α, β.

$$\begin{aligned}\phi_{eq}(\tau) &= -\frac{\beta q}{p}\left[\theta_u(\tau)\right]^{2-(p/q)},\\ \phi_{sw}(\tau) &= -\left[g_0(\tau)+g_1(\tau)\left|\theta_u(\tau)\right|+g_2(\tau)\left|\theta_v(\tau)\right|\right]\cdot \mathrm{sign}(\sigma(\tau)),\end{aligned} \tag{12}$$

and sign(·) is the sign function. The restrictions of system parameters are $\beta > 0$ and positive p, q are odd integers with $1 < p/q < 2$. The adaptive gains $g_i(\tau)$, $i = 0, 1, 2$ are respectively updated by the following algorithms.

$$\begin{aligned}\dot{g}_0(t) &= \gamma_0\left|\sigma(\tau)\right|\left|\theta_u(\tau)\right|^{(p/q)-1}, g_o(0)=0, \gamma_0>0\\ \dot{g}_1(t) &= \gamma_1\left|\sigma(\tau)\right|\left|\theta_u(\tau)\right|^{p/q}, g_1(0)=0, \gamma_1>0\\ \dot{g}_2(t) &= \gamma_2\left|\sigma(\tau)\right|\left|\theta_u(\tau)\right|^{(p/q)-1}\left|\theta_v(\tau)\right|, g_2(0)=0, \gamma_2>0\end{aligned} \tag{13}$$

Then, the synchronous error states $\theta_u(\tau)$, $\theta_v(\tau)$ in Eq. (4) can approach $\sigma(\tau) = 0$ and remain constant, that is, $\dot{\sigma}(\tau)=0$. Then $\theta_u(\tau)$ is forced to tend to zero at a finite time in advance and $\theta_v(\tau)$ is stabilized exponentially as below. Finally, the state synchronous control problem of the two SFHN nerve cells of Eqs. (1) and (2) is solved.

Proof.

There are two steps to prove Theorem 2 on the basis of the Lapunov stability theory. First, the positive definite function, $V(\tau) \geq 0$, which consists of $\sigma(\tau)$ and $g_i(\tau)$, $i = 0, 1, 2$, is selected. Then, it is proven that the selected positive definite function is a decreasing function, that is, $\dot{V}(\tau) < 0$. Finally, it is ensured that $\sigma(\tau) = 0$ and $g_i(\tau)$, $i = 0, 1, 2$ are converging to fixed values.

The positive definite function is selected as

$$V(\tau)=\frac{1}{2}\sigma^2(\tau)+\sum_{i=0}^{2}\frac{p}{2q\gamma_i}(g_i(\tau)-G_i)^2\geq 0, \tag{14}$$

where $G_i > 0$, $i = 0, 1, 2$ and satisfies

$$\begin{aligned}G_0 &> I_0 + I_{0\_s} + I_m + I_s + \left|\Delta(u_1,u_2)\right| + \left|d(\tau)\right|,\\ G_1 &> M_1 + M_2 + \alpha q/p + a,\\ G_2 &> 1.\end{aligned} \tag{15}$$

Taking the derivative of Eq. (14) vs τ combined with the dynamical system in Eq. (4), the defined IFFSSM in Eq. (8), and the adaptive control scheme in Eqs. (12) and (13), we obtain

$$\begin{aligned}\dot{V}(\tau) &= \sigma(\tau)\dot{\sigma}(\tau) + \sum_{i=0}^{2}\frac{p}{q\gamma_i}(g_i(\tau)-G_i)\dot{g}_i(\tau)\\ &= \sigma\left[\frac{p}{q}\left[\theta_u\right]^{p/q-1}\dot{\theta}_u + \alpha\left[\theta_u\right]^{p/q} + \frac{\beta}{c}\left(\frac{\dot{\theta}_v}{b}+\theta_v\right)\right] + \frac{p}{q}\sum_{i=0}^{2}\frac{g_i(\tau)-G_i}{\gamma_i}\dot{g}_i(\tau)\end{aligned}$$

$$\begin{aligned}\Rightarrow \dot{V}(\tau) = \sigma\frac{p}{q}\left[\theta_u\right]^{p/q-1}\cdot\Bigg[&\left(-F_1(x_1,x_2)+F_2(x_1,x_2)+\frac{\alpha q}{p}-a\right)\theta_u-\theta_v\\ &+(I_{0\_s}-I_0)+I_s\cos(\omega_s\tau)-I_m\cos(\omega_m\tau)-\Delta(u_1,u_2)-d(\tau)\\ &-\left(g_0(\tau)+g_1(\tau)\left|\theta_u\right|+g_2(\tau)\left|\theta_v\right|\right)\cdot\mathrm{sign}(\sigma)\Bigg]\\ &+\frac{p}{q}\sum_{i=0}^{2}\frac{g_i(\tau)-G_i}{\gamma_i}\dot{g}_i(\tau)\end{aligned} \tag{16}$$

$$\begin{aligned}\Rightarrow \dot{V}(\tau) \le \frac{p}{q}\left|\theta_u\right|^{p/q-1}\left|\sigma\right|\cdot\Big[&-\left(G_0-I_{0\_s}-I_0-I_s-I_m-\left|\Delta\right|-\left|d(\tau)\right|\right)\\ &-\left(G_1-M_1-M_2-\alpha q/p-a\right)\left|\theta_u\right|-\left(G_2-1\right)\left|\theta_v\right|\Big] < 0.\end{aligned} \tag{17}$$

Up to this stage, it is proven that the positive definite function, Eq. (14), is a decreasing function, which confirms that $\sigma = 0$ and $g_i(\tau) = G_i > 0$, $i = 0, 1, 2$ are guaranteed. By applying the proposed scheme in Eqs. (12) with (13), it is shown that $\theta_u(\tau)$, $\theta_v(\tau)$ of the dynamical system in Eq. (4) are asymptotically converging to $\sigma(\tau) = 0$ and maintaining $\dot{\sigma}(\tau) = 0$ from the given $\theta_u(0)$, $\theta_v(0)$.

Besides, with $\sigma(\tau) = 0$, $\theta_u(\tau)$ is stabilized in advance at a finite time τ_s using Eq. (9) with suitably selected values of $\alpha, \beta > 0$ and the positive odd integers p and q with $1 < p/q < 2$. Then, for $\theta_v(\tau)$, the exponential stabilization is achieved according to Theorem 1. Finally, the state synchronous control problem between the two SFHN nerve cells of Eqs. (1) and (2) is solved. This completes the proof.

Remark 3.

The control scheme in Eq. (12) includes the discontinuous term, i.e., the sign function sign(·). For the implementation of control input and to diminish the chattering phenomenon, sign(·) in Eq. (12) is replaced by $\tanh(\sigma/\delta)$ with a small constant of $\delta = 10^{-6}$.

4. Numerical Experiments

At present, the existing hardware implementation of neuronal circuits is a mature technology. Before the future practical realization of our proposed control scheme, its validation and feasibility are required. The preceding numerical experiments can provide the support for the implementation of neuronal circuits with voltage-sensing equipment.

In the following section, the numerical experiments for the two SFHN nerve cells of Eqs. (1) and (2) are performed for the developed adaptive IFFSSM control. The Runge–Kutta numerical solver for the differential equations with a time-step size of 10^{-4} is applied in the computation.

The initial conditions $(u_1, v_1) = (-0.25, 0.8)$, $(u_2, v_2) = (0.25, 0.5)$ are set in sequence. The positive constants of the nerve cell system are $a = 0.25$, $b = 0.02$, $c = 0.25$. Different amplitudes and frequencies of the EESs for the master and slave SFHN nerve cell systems are taken as $I_m = 0.055$, $\omega_m = 0.1$, $I_s = 0.06$, $\omega_s = 0.15$. The ionic currents applied to the two SFHN nerve cell systems are set as $I_{0\_s} = 0.082$ and $I_0 = 0.1$, respectively. The external disturbance and the system uncertainty of the master nerve cell are modeled by $d(\tau) = 0.25 \cdot \sin(0.1\pi\tau)$ and $\Delta(u_1, v_1) = 0.5 \cdot \sin(u_1)\sin(v_1)$, respectively.

The first numerical experiment with the positive design parameters of $p = 13$, $q = 11$, $\alpha = 0.6$, $\beta = 1.5$, $\gamma_0 = 0.0015$, $\gamma_1 = 0.001$, $\gamma_2 = 0.01$ for the adaptive IFFSSM control system in Eq. (4) associated with Eqs. (12) and (13) is proposed. The control input at $\tau = 0$ triggers the state synchronization between two nerve cells. The responses of IFFSSM $\sigma(\tau)$ with respect to the synchronous errors $\theta_u(\tau)$ and $\theta_v(\tau)$ are shown in Fig. 2. It is depicted that, when $\sigma(\tau) = 0$ is maintained, $\theta_u(\tau)$ tends to zero in a finite time in advance. Next, $\theta_v(\tau)$ approaches zero when $\sigma(\tau) = 0$ and $\theta_u = 0$. The stable characteristics of the defined IFFSSM in Eq. (8) with Theorem 1 are verified. In Fig. 3, the responses of $\theta_u(\tau)$ and $\theta_v(\tau)$ vs τ are depicted. It is shown that $\theta_u(\tau)$ tends to zero faster than $\theta_v(\tau)$ converges to zero. Nevertheless, the performance of control in this experiment is unacceptable owing to the convergent process in $\theta_v(\tau) \rightarrow 0$ being sustained for a considerably long time.

Indeed, the performance of control is modified by suitably adjusting the designed parameter α. For the same initial conditions, system parameters, and other designed parameters, except for α, as in the first experiment, the state trajectories corresponding to three values of α in the phase plane are depicted in Fig. 4. It is demonstrated that, for the larger value of α, $\theta_u(\tau)$ more quickly approaches zero in advance when the state trajectories start to stay on $\sigma(\tau) = 0$. Then, $\theta_v(\tau)$ is sequentially convergent. By selecting a smaller value of α, almost identical convergences of $\theta_u(\tau)$ and $\theta_v(\tau)$ are achieved. It is shown that the performance of control is improved by choosing a suitable value of α.

The second numerical experiment is conducted under the same simulation conditions as in the first experiment except for choosing $\alpha = 0.45$. In Figs. 5 and 6, the responses of $\theta_u(\tau)$, $\theta_v(\tau)$

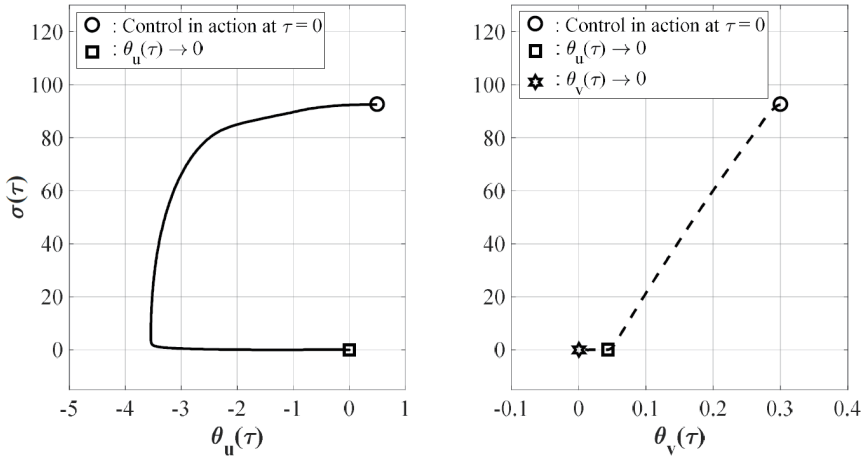

Fig. 2. Responses of $\sigma(\tau)$ versus $\theta_u(\tau)$ and $\theta_v(\tau)$ for $\alpha = 0.6$.

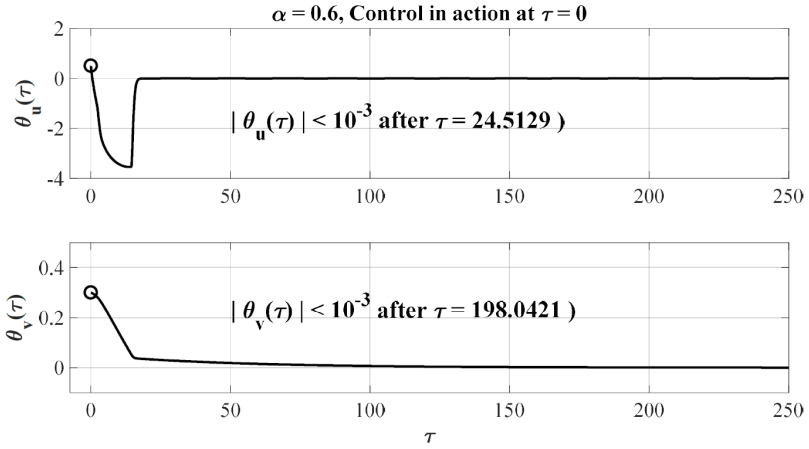

Fig. 3. Time responses of $\theta_u(\tau)$ and $\theta_v(\tau)$ for $\alpha = 0.6$.

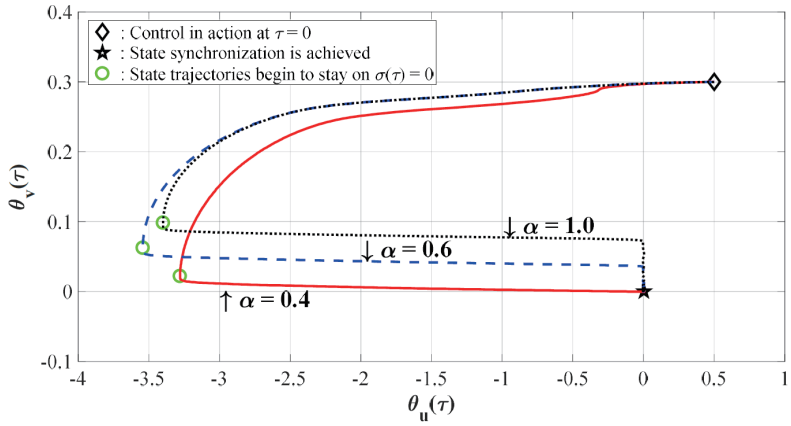

Fig. 4. (Color online) State trajectories for various values of α.

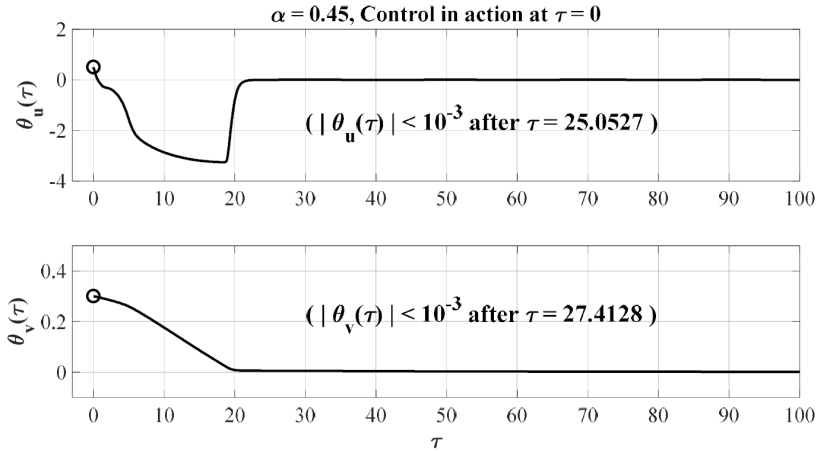

Fig. 5. Time responses of $\theta_u(\tau)$ and $\theta_v(\tau)$ for $\alpha = 0.45$.

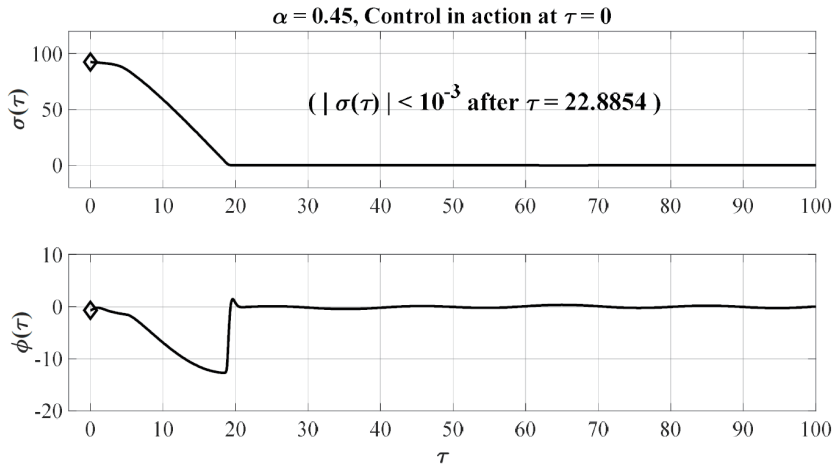

Fig. 6. Time responses of $\sigma(\tau)$ and $\phi(\tau)$ for $\alpha = 0.45$.

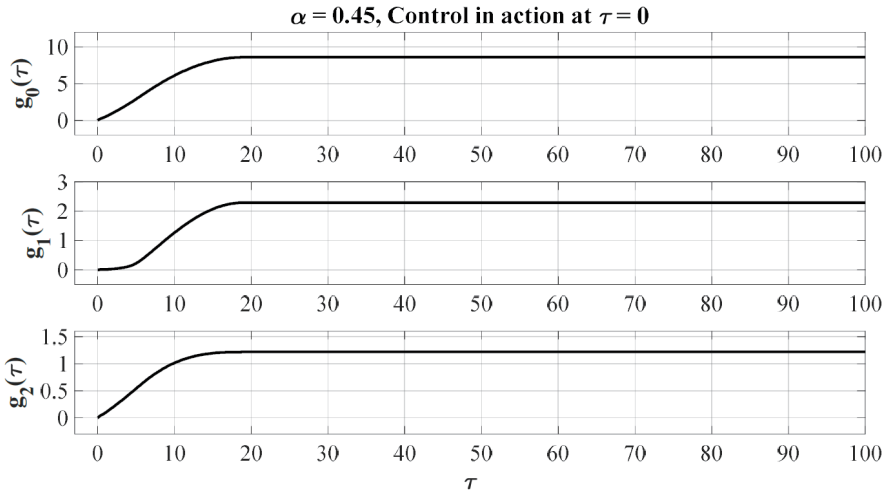

Fig. 7. Time responses of $g_i(\tau)$, $i = 0, 1, 2$ for $\alpha = 0.45$.

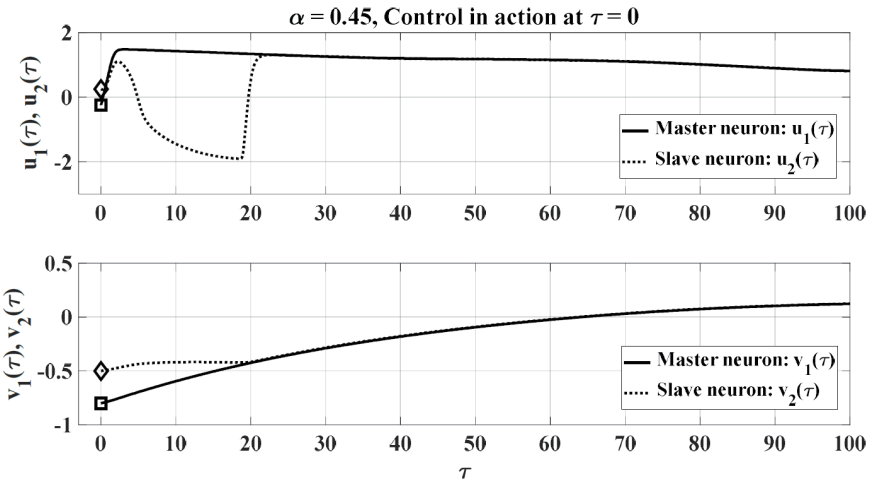

Fig. 8. Time responses of state variables for two SFHN nerve cells.

and the IFFSSM $\sigma(\tau)$ and the control input signal $\phi(\tau)$ vs τ are shown, respectively. It is shown that $\theta_u(\tau)$ and $\theta_v(\tau)$ have nearly identical convergence to the origin while $\sigma(\tau) = 0$ is held, and good performance of control is achieved. In addition, the control signal $\phi(\tau)$ of the proposed adaptive IFFSSM control is continuous without chatter.

The responses of three adaptive feedback gains vs τ are depicted in Fig. 7, and the gains are seen to finally become constant. It is indicated that $\theta_u(\tau)$, $\theta_v(\tau)$, and the IFFSSM $\sigma(\tau)$ all tend to zero in accordance with the adaption algorithms in Eq. (13). In Fig. 8, the responses of state variables vs τ for two SFHN nerve cells are shown. It is apparent that the state synchronous control problem in the presence of external disturbances and system uncertainties is solved.

5. Conclusions

The novel adaptive IFFSSM control scheme with robustness has been developed to solve the state synchronous control problem between two SFHN nerve cell systems in this study. The IFFSSM is defined by the proportional, the fractional powered, and the integral terms of state variables. Additionally, the special stability property, in which two state variables are stabilized in sequence on the sliding surface, is described. Two theorems that support the stability of the controlled system are provided and proven in the framework of the Lyapunov stability theory. For the future practical realization of the present control scheme in neuronal circuits, the proposed scheme is validated through numerical experiments.

Acknowledgments

We acknowledge the support of the School of Physics and Telecommunication Engineering, Yulin Normal University. This research was funded in part by the Scientific Research Fund Project (Grants: G2020ZK15, G2020ZK16, and G2021ZK19) of Yulin Normal University and the Major Cooperative Project (Grant: YLSXZD2019015) of Yulin Municipal Government and Yulin Normal University.

References

1 Y. Z. Liu, Y. Y. Xie, Y. C. Ye, J. P. Zhang, S. J. Wang, Y. Liu, G. F. Pan, and J. L. Zhang: IEEE Photonics J. **9** (2017) 7900512. https://doi.org/10.1109/JPHOT.2016.2639291
2 Z. Wu, X. Zhang, and X. Zhong: IEEE Access **7** (2019) 37989. https://doi.org/10.1109/ACCESS.2019.2906770
3 U. E. Kocamaz, B. Cevher, and Y. Uyaroglu: Chaos, Solitons Fractals **105** (2017) 92. https://doi.org/10.1016/j.chaos.2017.10.008
4 Z. Zhao, X. Li, J. Zhang, and Y. Pei: Int. J. Biomath. **10** (2017) 1750041. https://doi.org/10.1142/S1793524517500413
5 H. Y. Chen, K. C Wang, H. C Shen, and C. H. Yang: Microsyst. Technol. **27** (2021) 1107. https://doi.org/10.1007/s00542-018-4088-7
6 C. H. Yang, K. C. Wang, and L. Wu: Sens. Mater. **32** (2020) 3343. https://doi.org/10.18494/SAM.2020.2918
7 C. C. Yang and C. L. Lin: Nonlinear Dyn. **69** (2012) 2089. https://doi.org/10.1007/s11071-012-0410-6
8 C. Lu and X. Chen: J. Comp. Nonlinear Dyn. **11** (2016) 041011. https://doi.org/10.1115/1.4032074
9 M. Masoliver and C. Masoller: Sci. Rep. **8** (2018) 8276. https://doi.org/10.1038/s41598-018-26618-8
10 D. Yu, X. Zhou, G. Wang, Q. Ding, T. Li, and Y. Jia: Cognit. Neurodyn. **16** (2022) 887. https://doi.org/10.1007/s11571-021-09743-5
11 D. Yu, G. Wang, Q. Ding, T. Li, and Y. Jia: Chaos, Solitons Fractals **157** (2022) 111929. https://doi.org/10.1016/j.chaos.2022.111929

12 D. Q. Wei, X. S. Luo, B. Zhang, and Y.H. Qin: Nonlinear Anal. Real World Appl. **11** (2010) 1752. https://doi.org/10.1016/j.nonrwa.2009.03.029
13 T. W. Lai, J. S. Lin, T. L. Liao, and J. J. Yan: Adaptive Chaos Synchronization of FitzHugh-Nagumo Neurons, J. W. Park, T. G. Kim, and Y. B. Kim, Eds. (Springer, Berlin, Heidelberg, 2007) Communications in Computer and Information Science, vol. 5. 142–150.
14 H. T. Yu and J. Wang: Acta Phys. Chim. Sin. **62** (2013) 170511. https://doi.org/10.7498/aps.62.170511
15 M. Rehan and K. S. Hong: Phys. Lett. A **375** (2011) 1666. https://doi.org/10.1016/j.physleta.2011.03.012
16 Q. Zhang: Chaos, Solitons Fractals **58** (2014) 22. http://dx.doi.org/10.1016/j.chaos.2013.11.002
17 D. Fan, X. Song, and F. Liao: Int. J. Bifurcation Chaos **28** (2018) 1850031. https://doi.org/10.1142/S0218127418500311
18 Y. Zhang, C. Wang, J. Tang, J. Ma, and G. Ren: Sci. China Technol. Sci. **63** (2020) 2328. https://doi.org/10.1007/s11431-019-1547-5
19 X. F. Zhang, J. Ma, Y. Xu, and G. D. Ren: Acta Phys. Chim. Sin. **70** (2021) 090502. https://doi.org/10.7498/aps.70.20201953
20 M. M. Ibrahim, M. A. Kamran, M. M. N. Mannan, I. H. Jung, and S. Kim: Sci. Rep. **11** (2021) 3884. https://doi.org/10.1038/s41598-021-82886-x
21 Y. Wang, F. Mina, Y. Cheng, and Y. Dou: Eur. Phys. J. Spec. Top. **230** (2021) 1751. https://doi.org/10.1140/epjs/s11734-021-00121-0
22 I. Hussain, S. Jafari, D. Ghosh, and M. Perc: Nonlinear Dyn. **104** (2021) 2711. https://doi.org/10.1007/s11071-021-06427-x
23 H. C. Tuckwell and J. Jost: Physica A **388** (2009) 4115. https://doi.org/10.1016/j.physa.2009.06.029
24 B. Bao, A. Hu, H. Bao, Q. Xu, M. Chen, and H. Wu: Complexity **2018** (2018) 3872573. https://doi.org/10.1155/2018/3872573
25 D. Yang: Commun. Nonlinear Sci. Numer. Simul. **18** (2013) 2783. http://dx.doi.org/10.1016/j.cnsns.2013.02.004
26 M. M. Ibrahim and H. Jung: IEEE Access **7** (2019) 57894. https://doi.org/10.1109/ACCESS.2019.2913872
27 C. J. Thompson, D. C. Bardos, Y. S. Yang, and K. H. Joyner: Chaos, Solitons Fractals **10** (1999) 1825. https://doi.org/10.1016/S0960-0779(98)00131-3
28 Y. Gao: Chaos, Solitons Fractals **21** (2004) 943. https://doi.org/10.1016/j.chaos.2003.12.033
29 L. Luo: Science **373** (2021) 6559. https://doi.org/10.1126/science.abg7285
30 K. Shaukat, S. Luo, V. Varadharajan, I. A. Hameed, S. Chen, D. Liu, and J. Li: Energies **13** (2020) 2509. https://doi.org/10.3390/en13102509
31 Z. Liu, C. Wang, W. Jin, and J. Ma: Nonlinear Dyn. **97** (2019) 2661. https://doi.org/10.1007/s11071-019-05155-7
32 A. Tamaševicius, G. Mykolaitis, E. Tamaševiciute, and S. Bumeliene: Nonlinear Dyn. **81** (2015) 783. https://doi.org/10.1007/s11071-015-2028-y
33 Q. Xu and D. Zhu: IETE Tech. Rev. **38** (2021) 563. https://doi.org/10.1080/02564602.2020.1800526
34 D. Rajasekharan, A. Gaidhane, A. R. Trivedi, and Y. S. Chauhan: IEEE Trans. Comput. Aided Des. Integr. Circuits Syst. **41** (2022) 2107. https://doi.org/10.1109/TCAD.2021.3101407
35 Y. Liu, W. J. Xu, J. Ma, and F. Alzahrani, A. Hobiny: Front. Inform. Technol. Electron. Eng. **21** (2020) 1387. https://orcid.org/0000-0002-6127-000X
36 Y. Guo, C. Wang, Z. Yao, and Y. Xu: Physica A **602** (2022) 127644. https://doi.org/10.1016/j.physa.2022.127644
37 Y. Guo, P. Zhou, Z. Yao, and J. Ma: Nonlinear Dyn. **105** (2021) 3603. https://doi.org/10.1007/s11071-021-06770-z
38 M. Ge, L. Lu, Y. Xu, R. Mamatimin, Q. Pei, and Y. Jia: Chaos, Solitons Fractals **133** (2020) 109645. https://doi.org/10.1016/j.chaos.2020.109645
39 G. Wang, Y. Xu, M. Ge, L. Lu, and Y. Jia: AEU Int. J. Electron. Commun. **120** (2020) 153209. https://doi.org/10.1016/j.aeue.2020.153209
40 Y. Zhang, Y. Xu, Z. Yao, and J. Ma: Nonlinear Dyn. **102** (2020) 1849. https://doi.org/10.1007/s11071-020-05991-y
41 X. Yu and Z. Man: IEEE Trans. Circuits Syst. I Regul. Pap. **49** (2002) 261. https://doi.org/10.1109/81.983876